Automatic Detection of Mitral Annulus in Echocardiography based on Prior Knowledge and Local Context

Wei Song[1], Wei Xu[1], Xin Yang[1], Liping Yao[2], Kun Sun[2]

[1]Institution of Image Processing and Pattern Recognition, Shanghai Jiao Tong University, Shanghai, China
[2]Xinhua Hospital, School of Medicine, Shanghai Jiao Tong University, Shanghai, China

Abstract

Due to the inherent noisy, low resolution and limited imaging range of echocardiography, it is difficult to identify mitral annulus (MA) where valves end that is crucial for further segmentation, modeling and multi-modalities registration of mitral valves. This work aims to automatically detect MA hinge points combining information of intra-cardiac local context and location relationships. The method includes the following steps: (1) segment left ventricle (LV) by prior shape and local histogram fitting based Active Contour Model (ACM); (2) design the local context features for training and classification of MA hinge points; (3) utilize additive min kernel based Support Vector Machines (SVM) classifier for fast computation to obtain MA candidates; (4) estimate MA hinge points by K-means algorithm under the location constraint of LV and MA. Our method was tested on echocardiographic four chamber image sequence of 10 pediatric patients (6 boys, 4 girls, 7.6 $\pm$ 3.4 years). Compared with the manual annotations, the automatically detected MA results are reliable with reasonable accuracy, for lateral point (2.0 $\pm$1.9, 1.8 $\pm$ 1.2) pixels and for septal point (2.9 $\pm$2.6, 1.2 $\pm$1.0) pixels.

1. Introduction

The mitral annulus (MA) is an essential intra-cardiac structure defined as a saddle shape that anchors the mitral valves. Studies on MA geometry have shown potential values in the assessment of mitral function, pathological diagnosis, surgical valve reconstruction planning, and model simulating.

Detection and segmentation of MA are the crucial pre-procedure for MA analysis [1, 2]. [3] suggested an automated tracking method of MA motion using dynamic programming. [4] introduced graph cut to segment MA in 3D echocardiography. [5] proposed a patient-specific modeling and quantification of mitral valves combining thin tissue detector and active contour model (ACM). [6] utilized learning algorithm to segment aortic and mitral valves in a cardiac cycle from CT and TEE.

This work presents an automatic detection method of MA hinge points. First, left ventricle is segmented using ACM based on prior shape and local histogram fitting. Then MA hinge points are detected by additive Support Vector Machines (SVM) classifier from local context features and prior location constraint of LV and MA.

2. Method

2.1. Left ventricle segmentation

Our method of LV segmentation applies prior LV shape and local histogram fitting based ACM.

Learning a LV shape model includes registration and modeling of LV prior shape set. The signed distance function based rigid registration method in [7] is used to align shape training set to obtain a aligned shape set denoted by $\{\varphi_i(\mathbf{u})\}_{i=1,\ldots,n}$, where $\mathbf{u}=(u,v)$ is the coordinates of shape space. Then PCA is utilized to transfer modeling from shape φ to parameter $\boldsymbol{\gamma}$: $\boldsymbol{\gamma} = U_k^T(\bar{\varphi} - \varphi)$, where U_k is a $d \times k$ matrix comprising top k largest eigenvector with the cumulative > 95%.

Kernel density estimation (KDE) is a powerful nonparametric technique to model the shape variation [8] that allows to approximate arbitrary distributions. The distribution of parameter $\boldsymbol{\gamma}$ is obtained by KDE from the training shape set $\{\boldsymbol{\gamma}_i\}_{i=1,\mathrm{K},n}$.

$$P(\boldsymbol{\gamma}) \propto \frac{1}{n}\sum_{i=1}^{n}\exp\left(-\frac{1}{2\sigma^2}d^2(\boldsymbol{\gamma},\boldsymbol{\gamma}_i)\right)$$

where d^2 is the Euclidean distance and σ is the kernel width given by $\sigma^2 = \frac{w_S}{n}\sum_{i=1}^{n}\min_{j\neq i} d^2(\boldsymbol{\gamma}_i,\boldsymbol{\gamma}_j)$, w_S is a constant to adjust the kernel width. The energy function of reconstruction in $\boldsymbol{\gamma}$ is given by $E_\gamma(\boldsymbol{\gamma}) = -\log P(\boldsymbol{\gamma})$. The

gradient descent equation can be written as:

$$\frac{\partial \boldsymbol{\gamma}}{\partial t} = \sum_{i=1}^{n} w_{Si} \frac{\partial}{\partial \boldsymbol{\gamma}} d^2(\boldsymbol{\gamma}, \boldsymbol{\gamma}_i) \Big/ 2\sigma^2 \sum_{i=1}^{n} w_{Si}$$

where w_{Si} is the shape force weight of $\boldsymbol{\gamma}_i$.

$$w_{Si} = \exp\left(-\frac{1}{2\sigma^2} d^2(\boldsymbol{\gamma}, \boldsymbol{\gamma}_i) \right)$$

The iteration is stop till its convergence. The obtained prior shape model then is applied to guild the curve evolution in ACM.

Local fitting energy function is proposed to segment regions with hard-predefined distributions [9]. Then Liu et al presented a nonparametric region-driven ACM using local histogram fitting energy [10]. The energy function is defined as:

$$\begin{aligned} E(\phi, P_i^{\mathbf{x}}, P_o^{\mathbf{x}}) &= \int_\Omega \left| \nabla H(\phi(\mathbf{x})) \right| d\mathbf{x} \\ &+ \lambda \int_\Omega \int_\Omega H(\phi) K_\sigma(\mathbf{x}-\mathbf{y}) D(P_i^{\mathbf{x}}, P_r^{\mathbf{y}}) d\mathbf{y} d\mathbf{x} \\ &+ \lambda \int_\Omega \int_\Omega (1-H(\phi)) K_\sigma(\mathbf{x}-\mathbf{y}) D(P_o^{\mathbf{x}}, P_r^{\mathbf{y}}) d\mathbf{y} d\mathbf{x} \end{aligned}$$

where given a point $\mathbf{x} \in \Omega$, ϕ is the level set function. $P_i^{\mathbf{x}}$ and $P_o^{\mathbf{x}}$ are the fitting histograms approximate the distribution inside and outside the evolving curve at $\mathbf{x}$, respectively. $K_\sigma(\mathbf{x}\text{-}\mathbf{y})$ is Gaussian kernel function with variance $\sigma>0$. λ is a constant. $D(\cdot,\cdot)$ is the histogram distance. If Wasserstein distance used, first for a fixed level set function, the updating function of local fitting energy, namely local cumulative histogram are:

$$F_i^{\mathbf{x}}(z) = \frac{\int_\Omega H(\phi) K_\sigma(\mathbf{x}-\mathbf{y}) F_r^{\mathbf{y}}(z) d\mathbf{y}}{\int_\Omega H(\phi) K_\sigma(\mathbf{x}-\mathbf{y}) d\mathbf{y}}$$

$$F_o^{\mathbf{x}}(z) = \frac{\int_\Omega (1-H(\phi)) K_\sigma(\mathbf{x}-\mathbf{y}) F_r^{\mathbf{y}}(z) d\mathbf{y}}{\int_\Omega (1-H(\phi)) K_\sigma(\mathbf{x}-\mathbf{y}) d\mathbf{y}}$$

Then with fixed $F_i^{\mathbf{x}}$ and $F_o^{\mathbf{x}}$, the curve evolution function is obtained as follows by gradient descent:

$$\begin{aligned} \frac{\partial \phi}{\partial t} = \delta(\phi) \cdot \Bigg\{ & \nabla \cdot \left(\frac{\nabla \phi}{|\nabla \phi|} \right) - \lambda \int_\Omega K_\sigma(\mathbf{x}-\mathbf{y}) \\ & \times \int_0^R \left(\left| F_i^{\mathbf{x}}(z) - F_r^{\mathbf{y}}(z) \right| - \left| F_o^{\mathbf{x}}(z) - F_r^{\mathbf{y}}(z) \right| \right) dz d\mathbf{y} \Bigg\} \end{aligned}$$

Note that the larger σ, the more global information involved.

Then LV prior shape is combined into the local histogram fitting based ACM to balance the shape and local features. If Wasserstein distance used, the model minimizes

$$\begin{aligned} & \int_\Omega \left| \nabla H(\phi(\mathbf{x})) \right| d\mathbf{x} \\ & + \lambda \int_\Omega \int_\Omega H(\phi) K_\sigma(\mathbf{x}-\mathbf{y}) \int_0^R \left| F_i^{\mathbf{x}}(z) - F_r^{\mathbf{y}}(z) \right| dz d\mathbf{y} d\mathbf{x} \\ & + \lambda \int_\Omega \int_\Omega (1-H(\phi)) K_\sigma(\mathbf{x}-\mathbf{y}) \int_0^R \left| F_o^{\mathbf{x}}(z) - F_r^{\mathbf{y}}(z) \right| dz d\mathbf{y} d\mathbf{x} \\ & \text{s.t.} \int_\Omega \left(H(\phi) - H(\varphi(B)) \right)^2 d\mathbf{x} = \alpha \int_\Omega \delta(\varphi(B)) d\mathbf{x} \end{aligned}$$

where φ is the optimized shape model, and B is the backward transformation.

In order to avoid leaking out, an inequality of distance of local fitting histograms of current inner and outer curves is introduced to balance σ and local fitting histograms:

$$\int_0^R \left| F_i^{\mathbf{x}}(z) - F_o^{\mathbf{x}}(z) \right| dz < \varepsilon$$

when Wasserstein distance used. If it's satisfied, the current σ is enlarged. Solving the whole variational model has two stages to set different α values for convergence to a local minimum.

Meanwhile, two strategies are applied to speed up computation: SDF based fast level set algorithm [11] and grayscale compression [12].

2.2. Local context feature design

In the cross-sectional planes along the long axis direction, the junction points between the annulus and the leaflets are hinge points on the annulus [13].

Because of inherent noisy, low spatial resolution and limited imaging range, intra-cardiac structures may be edge-blurred and of similar intensities. The general image detectors fail in echocardiographic images. Meanwhile, spatial relationships of atrium and ventricle are fixed in the echocardiography. Therefore in this work, a local context feature is obtained for subsequent classification of MA hinge point candidates for intra-cardiac structures in echocardiography. Ideally, every pixel in the neighborhood can be put into context. However, this would generate a large feature space. Therefore, sparely sampling could enhance training and classification. In this work, the local context feature of a pixel is obtained from sparely sampling the context locations on eight rays in 45 degree intervals. A context location sequence {1, 3, 5, 8, 11, 15, 19, 23} is used for each ray. Their intensity and mean intensity in 3×3 window are chosen as features. These context features represent the local intra-cardiac configuration information of interest. Note that the context location sequence is different in specific applications.

2.3. Additive min kernel SVM classifier

Additive min kernel SVM classifier is applied to

obtain MA hinge point candidates from local context features. The basic concept of additive kernel SVM will be briefly described as follows. More details can be found in the reference [14].

Supposing the training data denoted by $\{(y_i, \boldsymbol{x}_i)\}_{i=1}^{N}$ with $y_i \in \{-1,1\}$, $x_i \in \boldsymbol{R}^n$, a C-SVM formulation is used here [15]. The min kernel is $K_{\min}(\boldsymbol{x}, \boldsymbol{z})$ defined as:

$$K_{\min}(\boldsymbol{x}, \boldsymbol{z}) = \sum_{i}^{n} \min(x_i, z_i)$$

The evaluating function of classification is

$$h(\boldsymbol{z}) = \sum_{l=1}^{m} \alpha_l y_l K_{\min}(\boldsymbol{z}, \boldsymbol{x}_l) + b = \sum_{l=1}^{m} \alpha_l y_l \sum_{i=1}^{n} \min(z_i, x_{l,i}) + b$$

The key property of min kernel exchanges the summation to obtain:

$$\begin{aligned} h(\boldsymbol{z}) &= \sum_{l=1}^{m} \alpha_l y_l \sum_{i=1}^{n} \min(z_i, x_{l,i}) + b \\ &= \sum_{i=1}^{n} \left(\sum_{l=1}^{m} \alpha_l y_l \min(z_i, x_{l,i}) \right) + b = \sum_{i=1}^{n} h_i(z_i) + b \end{aligned}$$

So the function $h(\cdot)$ can be rewritten as a sum of 1D functions $h_i(\cdot)$, where

$$h_i(s) = \sum_{l=1}^{m} \alpha_l y_l \min(s, x_{l,i})$$

This decomposition allows approximating each dimension function to gain the approximate solution of the classifier. Therefore, additive kernel SVM has advantages of nonlinearity and fast calculation.

2.4. Outline of method

The complete process of our method is summarized as follows:

(1) Register and learn of LV shape training set.
(2) Initialize the evolving curve and KDE shape model.
(3) Compress the grayscale to 25 and calculate $F_i^{\mathbf{x}}$ and $F_o^{\mathbf{x}}$ of each pixel.
(4) First stage: setting α=10.
(5) Optimize parameters of registration and shape model.
(6) Calculate Lagrange multiplier ζ.
(7) Check whether the inequality is satisfied to enlarge the kernel width and iterate evolving curve equation.
(8) Check whether convergence or maximum iterative number is reached. If not, go to (5).
(9) Second stage: setting α=0.2.
(10) Calculate Lagrange multiplier ζ.
(11) Check whether the inequality is satisfied to enlarge the kernel width and iterate evolving curve equation.
(12) Check whether convergence or maximum iterative number is reached. If not, go to (10).
(13) Training the additive min kernel SVM from local context feature set of MA.
(14) Classify and gain the MA candidates.
(15) Check whether the distance between MA candidate and LV is larger than the threshold. If yes, dismiss.
(16) Gain the clustering center as MA hinge points by K-means.

3. Experiments and results

RT3DE scanning is performed with a commercial available system (Sonos 7500, Philips, Co.) in Shanghai Children's Medical Center affiliated to Shanghai Jiao Tong University. The 3D echocardiograhy are formatted as 208×160×144 per frame. 10 normal young children (6 boys, 4 girls, 7.6±3.4 years) are selected in this work.

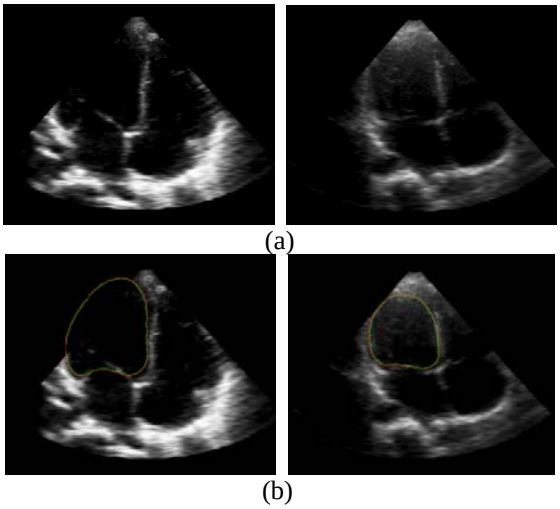

Figure 1. Segmentation of left ventricle in ultrasound images of the heart: (a) are the images to be segmented; (b) are the segmentation results using our method. The red contours correspond to the deformable shapes, and the green ones the evolving curves.

Figure 1-3 are results of LV segmentation, additive kernel SVM classification and clustering centers of K-means, respectively. The performance of our method is evaluated by comparison with manual segmentation with the errors summarized in Table 1. The results indicate that our method achieves acceptable accuracy.

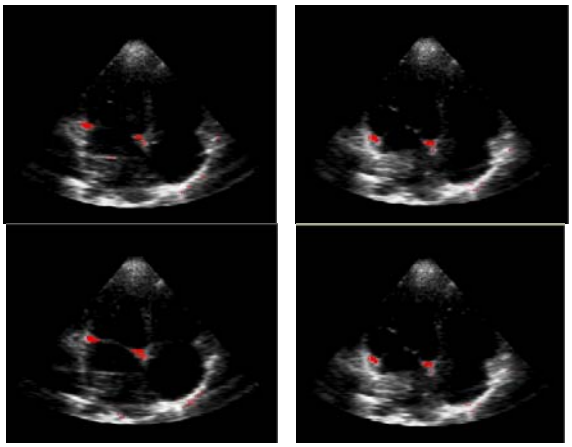

Figure 2. The results of additive min kernel based SVM classifier using local context features.

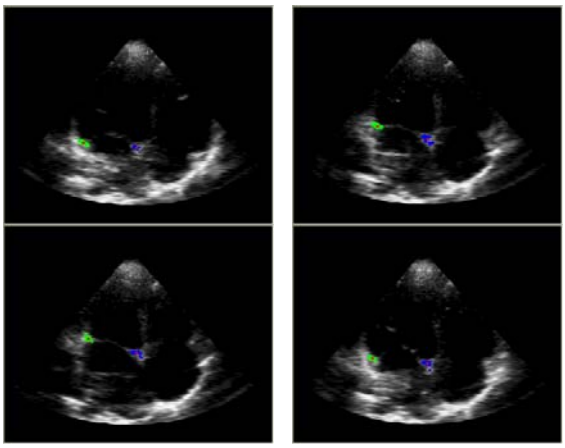

Figure 3. Automatic identification of mitral annular hinge points in a cardiac cycle (red points).

Table 1. Errors between our method and manual segmentation results.

	Lateral(left)				Septal(right)			
	x		y		x		y	
	mean	std	mean	std	mean	std	mean	std
pixel	2.0	1.9	1.8	1.2	2.9	2.6	1.2	1.0

4. Conclusions

This work provides an effective tool for automatic detection of MA hinge points in echocardiography that could support further mitral segmentation, modeling and multimodality registration.

Acknowledgements

This paper has been partially supported by National Basic Research Program of China (2010CB732506) and Shanghai Basic Research Program (12JC1406600).

References

[1] Pai RG, Bodenheimer MM, Pai SM, et al. Usefulness of systolic excursion of the mitral annulus as an index of left ventricular systolic function. The American Journal of Cardiology 1991; 67: 222–4.

[2] Wei Song, Xin Yang, Kun Sun. Quantitative analysis of 3D mitral complex geometry using support vector machines. Physiological Measurement 2012; 33: 1213-24.

[3] Nevo ST, van Stralen M, Vossepoel AM, et al. Automated tracking of the mitral valve annulus motion in apical echocardiographic images using multidimensional dynamic programming. Ultrasound Med Biol 2007; 33(9): 1389-99.

[4] Schneider RJ, Perrin DP, Vasilyev NV, et al. Mitral annulus segmentation from 3D ultrasound using graph cuts. IEEE transactions on Medical Imaging 2010; 29: 1676-87.

[5] Burlina P, Sprouse C, DeMenthon D, et al. Patient-specific modeling and analysis of the mitral valve using 3D-TEE. Lecture Notes in Computer Science 2010; 6135: 135-46.

[6] Ionasec RI, Voigt I, Georgescu B, et al. Patient-specific modeling and quantification of the aortic and mitral valves from 4-D cardiac CT and TEE. IEEE transactions on Medical Imaging 2010; 29(9): 1636-51.

[7] Paragios N, Rousson M, Ramesh V. Non-rigid registration using distance functions. Computer Vision and Image Understanding 2003; 89(2-3): 142-65.

[8] Cremers D, Osher SJ, Soatto S. Kernel density estimation and intrinsic alignment for shape priors in level set segmentation. International journal of computer vision 2006; 69(3): 335-51.

[9] Li C, Kao CY, Gore JC, et al. Minimization of region-scalable fitting energy for image segmentation. IEEE transactions on image processing 2008; 17(10): 1940-9.

[10] Liu WP, Shang YF, Yang X, et al. A shape prior constraint for implicit active contours. Pattern Recognition Letters 2011; 32(15): 1937-47.

[11] Shi Y, Karl WC. A real-time algorithm for the approximation of level-set-based curve evolution. IEEE transactions on image processing 2008; 17(5): 645-56.

[12] Ojala T, Pietikainen M, Maenpaa T. Multiresolution gray-scale and rotation invariant texture classification with local binary patterns. IEEE transactions on pattern analysis and machine intelligence 2002; 24(7): 971-87.

[13] Tu ZW and Bai X. Auto-context and its application to high-level vision tasks and 3D brain image segmentation. IEEE Transactions on Patten Analysis and Machine Intelligence 2010; 32(10): 1744-57.

[14] Maji S, Berg A. Malik J. Efficient classification for additive kernel SVMs. IEEE Transactions on Pattern Analysis and Machine Intelligence 2012; 35(1): 66-77.

[15] Burges CJC. A tutorial on support vector machines for pattern recognition. Data Mining and Knowledge Discovery 1998; 2: 121-67.

Address for correspondence.
Wei Song.
Room 220, No.2 SEIEE Building, Shanghai Jiao Tong University, No.800, Dong Chuan Road, Shanghai 200240, China
esong1029@hotmail.com
yangxin@sjtu.edu.cn